

EDGE DETECTION ALGORITHMS IN INTENSITY SAR IMAGES: EMPIRICAL COMPARISON OF PERFORMANCES AND PROPOSED IMPROVEMENTS

Ignacio Melgar, Sener Ingeniería y Sistemas, Spain, ignacio.melgar@sener.es
Juan Fombellida, Sener Ingeniería y Sistemas, Spain, juan.fombellida@sener.es
Jaime Gómez, Sener Ingeniería y Sistemas, Spain, jaime.gomez@sener.es
Juan Seijas, Universidad Politécnica de Madrid, Spain, seijas@gc.ssr.upm.es

ABSTRACT

Different edge-detection algorithms developed for high-speckle SAR images are evaluated and compared. Two evaluation criterions have been selected: (i) quality of the detected edges, specially considering false alarms, edge thickness and level of discontinuities on detected edges. (ii) computational efficiency. Some modifications on the best-performance algorithms regarding edge quality are proposed, at the expense of a certain computational load increase.

KEYWORDS: Synthetic Aperture Radar, edge detection, speckle, probability of false alarm, probability of detection, wavelet.

1. INTRODUCTION

Edge detection in SAR images is a preliminary processing step very common in image segmentation, infrastructures recognition, rural/urban area identification and image intelligence processes, as well as geometry-recognition based navigation techniques. During the last 20 years many edge detection algorithms have been developed. These algorithms can be classified in three main groups: sliding-window, based on wavelets and based on image segmentation. Edge detection algorithms can also be divided in two categories, depending on the nature of the input data: intensity images and single look complex (SLC) images. In this paper we focus our comparative study on the ones with input intensity images. All edge detection algorithms include two basic steps in their processing: (i) extraction of the Edge Strength Map (ESM) for each pixel of the image; (ii) application of a certain threshold to the map in order to decide if each pixel contains an edge or not. The ESM, when normalized from 0 to 1, can be considered for each pixel as the probability of presence of an edge in that pixel. Different algorithms differ in the different way ESMs and threshold values are obtained. We group those algorithms in three main families:

1.1 Sliding-window algorithms:

ROA [1] (Ratio of Averages): for each pixel of the image (PUT or Pixel Under Test), the two mean intensity on a certain fixed-length row wise or column wise window of pixels on each side of the PUT is computed. Then the edge strength value is normalized computing the minimum between the quotient of the two mean intensities and its inverse. The algorithm provides CFAR feature. Its main drawback is the assumption that windows on each side of the PUT do not contain edges when the PUT does.

White and Oliver operator [2]: in this case, the windows used to compute the mean intensity on each side of the PUT have configurable width and length varying from a minimum to a maximum value. Difference between means instead of minimum quotient is taken as edge strength value for each pixel, taking the highest obtained value through all different computed window lengths and directions (row-wise or column-wise). Then, a certain threshold is applied to detect edges. In this case, small windows will detect edges closed to each other while long windows may detect weaker edges between big homogeneous regions.

Likelihood Ratio operator (LR) of Oliver, Blacknell and White [3]: for a given vertical or horizontal one-pixel width window, the operator obtains the probability of presence of an edge on each of the central pixels of that window using a logarithmic likelihood ratio. Threshold value is obtained from the desired Pfa. In case of computing the probability only for the central pixel of the window, this operator is equivalent to the ROA operator. Due to this similarity, evaluation and comparison will only be performed on ROA operator.

Ratio Of Exponentially Weighted Averages operator (ROEWA) [4]: this algorithm applies an MMSE filter for the estimation of the local mean assuming a certain stochastic model of multiple edges and a multiplicative model of speckle. This filter is applied by one causal exponentially

negative transfer function and its time-inverted anti-causal version. In this way, for each pixel of the image, the exponentially weighted average on each side of the pixel (either vertically or horizontally computed) is obtained, and the operator is computed as the minimum between the quotient of the two averages and its inverse. Once the operator has been computed horizontally and vertically for each pixel, final ESM is obtained as the square root of the squares of the vertical and horizontal values.

Ratio of Difference and Minimum Averages (RDMA) [5]: similar to ROA, but in this case the operator is obtained as the difference of average intensities divided by the minimum of both averages. Identically to the ROA case, RDMA values are computed horizontally and vertically for each pixel, and final ESM value is obtained as the square root of the squares of the vertical and horizontal values. The authors propose then two algorithms for discrimination of edge and non-edge pixels: Non-Zero Crossing Suppression (NZCS) and Non-Local Maxima Suppression (NLMS). The implementation and test of both algorithms have driven us to results with high false detection rates, so the selected approach for this case has been to compute the ESM using the RDMA operator, and then to apply a threshold value like in all other cases.

Other authors propose sliding-window algorithms with SLC input data. These are based on the statistically optimum detection adapted to the correlated nature of the SAR clutter. Two of them are the Spatially Whitening Filter–Likelihood Ratio operator [6,7] and the Improved Multi-Edge Likelihood Ratio operator [8]. This paper is dedicated to input intensity images algorithms, results for algorithms with SLC inputs are studied in another paper under elaboration.

1.2 Wavelet-based algorithms:

Zhiqin, Chunlin, Jianguo and Shunji propose in [9] a wavelet-based edge detection algorithm conceived to mitigate edges produced by speckle and enhance edges produced by differences in textures. This mitigation is performed by the Adaptive Fuzzy Weighted Median Filter. The algorithm description did not allow a reliable implementation, so could not be considered in this comparative study.

Fjørtoft, Marthon and Lopès wavelet-based edge detector [10]: this algorithm obtains the wavelet transform of the input image for a given decomposition level, and applies the ROA operator as defined in [1] for a certain set of window sizes. The final ESM is obtained for each pixel combining the ESM ROA results for each window size. Authors propose two combination methods: maximum ESM selection and mean ESM selection. Then, a threshold is applied, and erosion methods or watershed-based methods are suggested to reduce false-edge rate. These last steps have been removed from the processing to compare algorithms in similar conditions.

Madchakham, Thitimajshima and Rangsanseri's wavelet-based edge detector [11]: the algorithm assumes a multiplicative speckle model, and uses the logarithm to convert it in additive noise. Then, it computes the overcomplete wavelet transform (no down-sampling) on a certain decomposition level, and applies a soft threshold to each subband (horizontal and vertical), obtaining the ESM as the modulus of both soft-thresholded subbands. The last step of the processing applies a threshold and removes all pixel edges with direction different from the edge direction of the nearest ESM local maximum. This step has not been implemented due to certain missing definitions, and a threshold is applied to the ESM as in all previous cases. Haar mother wavelet has also been assumed.

Two other edge detection algorithms for SAR images based on the wavelet transform were proposed by Manian, and Vásquez [12] as well as by Chabert, Tournere and Mesnager [13]. These algorithms are not included in the comparison, due to the fact that their description is too generic to allow a reliable implementation.

1.3 Segmentation-based algorithms

Moreels and Smrekar in [14] as well as Marthon, Paci and Cubero-Castan in [15] proposed two Watershed-based algorithms, in which the image is segmented by different textures, and edge pixels are declared in the boundary regions of image segments. Due to their different processing, these algorithms are not included to be compared with the others.

Summarising, the comparison performed in this paper is based on the quality of the ESM, which might be directly extrapolated to the false-edge rate. To optimise uniformity, no erosion and growing techniques have been implemented, because those could be applied to all of presented algorithms to improve performance. After all the considerations detailed in previous paragraphs, algorithms described in [1], [2], [4], [5], [10] and [11] are the ones compared in this paper.

2. ALGORITHM PERFORMANCES AND PROPOSED IMPROVEMENTS



Figure 1: Original SAR image

Figure 1 contains the original intensity SAR image that will be used for algorithm evaluation. It mixes speckled rural areas, in which different country fields can be identified, with urban areas. The results obtained from execution of all edge detection algorithms to be compared in this paper are shown in next figures. Results correspond to the best possible values of their input parameters, specified under each figure. For each experiment, two images are provided as results: ESM image (left), and binary edge detection image (right) obtained after applying a certain threshold to that ESM image. Thresholds are obtained from ESM percentile values, any pixel greater than the threshold will be considered an edge pixel (plotted in green).



Figure 2: ROA operator, window size 17x17. Left: ESM. Right: edges with 85% percentile.

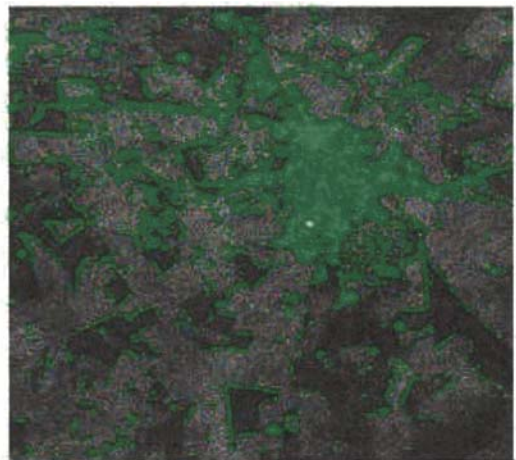


Figure 3: Oliver & White operator, window sizes in pixels: minimum 5, fixed 13 and maximum 17. Left: ESM. Right: detected edges with 85% percentile.

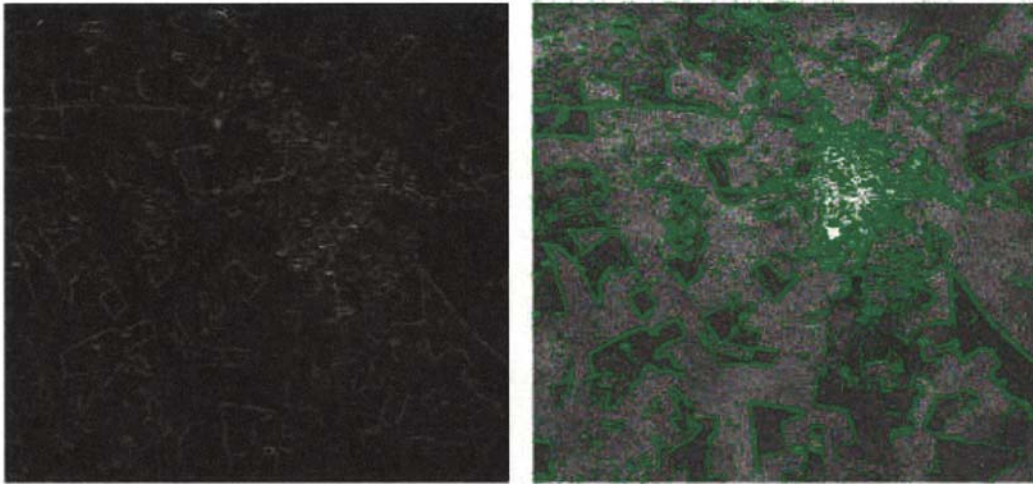


Figure 4: ROEWA operator, filter constant 0,02. Left: ESM. Right: edges with 85% percentile.

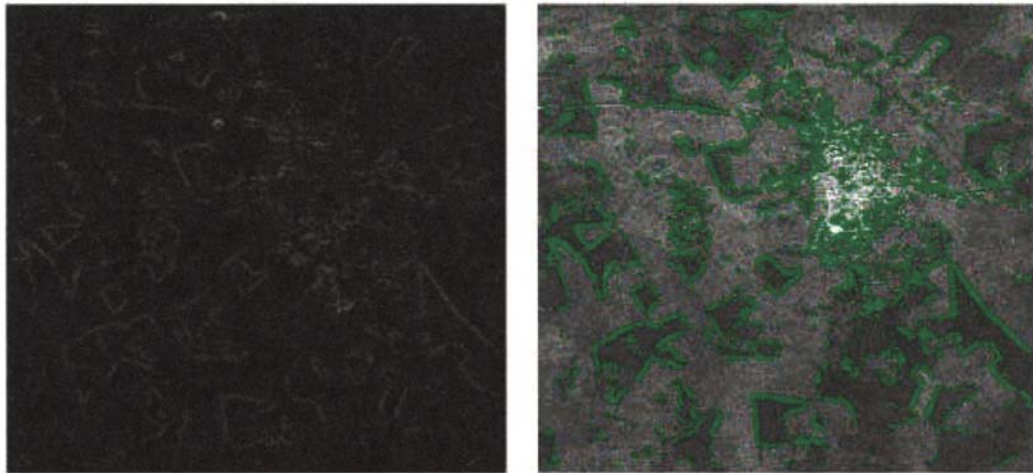


Figure 5: RDMA operator, window size 51. Left: ESM. Right: edges with 90% percentile.

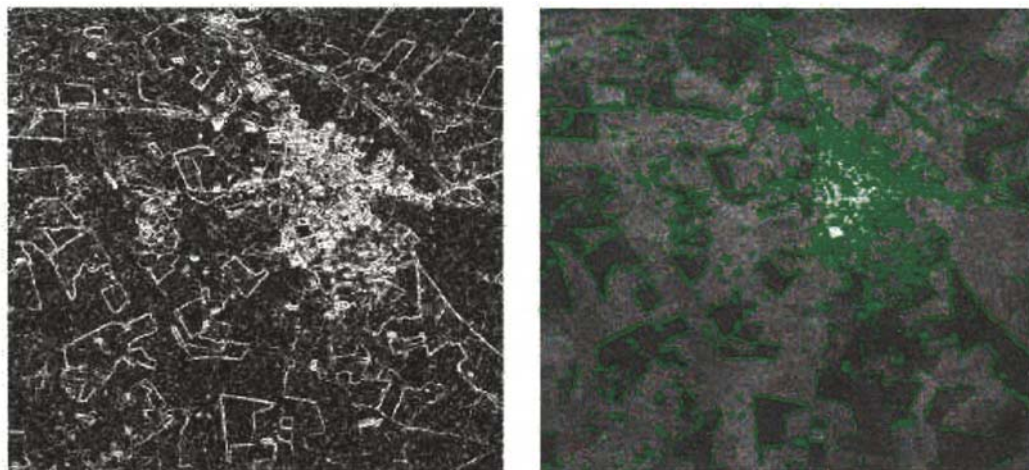


Figure 6: Madchakham algorithm, wavelet scale: 4.
Left: ESM. Right: edges with 90% percentile.

Next figure contains the results obtained for an improved variant of the Multiresolution ROA algorithm ([10]). As it was mentioned, two strategies to combine the ESMs obtained from ROA for each selected window size were proposed by the authors of [10]: mean and maximum. We propose the following improvement: to combine ESMs pixel by pixel with the minimum. With

this approach, one large window size can be used to obtain an ESM with thick edges and low false alarm rate, and another reduced window size can be used to obtain a ESM with thin edges and higher false alarm rate. The minimum of both ESMs will maintain low false alarm rate and low edge thickness:

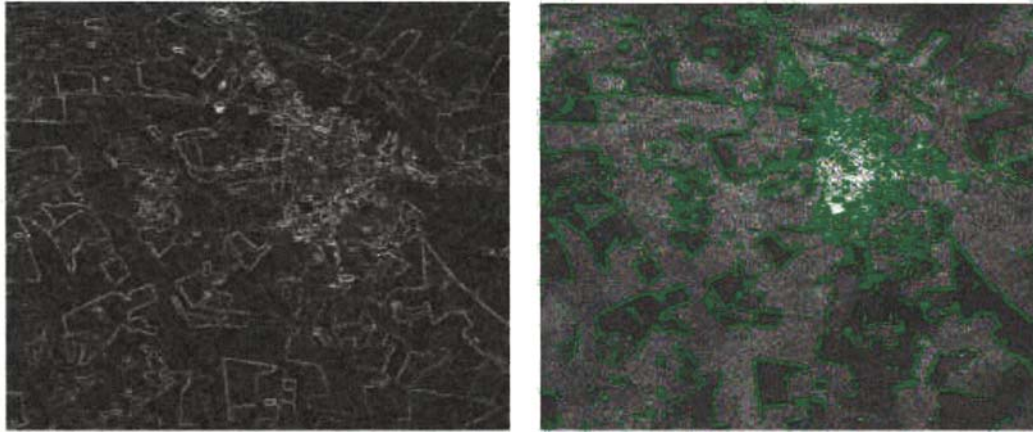


Figure 7: Multiresolution ROA algorithm, combination with minimum, wavelet scale 3, ROA sizes 5, 10 and 15. Left: ESM. Right: edges with 90% percentile.

3. QUALITATIVE COMPARISON AND COMPUTATIONAL LOAD

Next table contains a summary of the performance in terms of advantages, disadvantages and computational load detected on all evaluated algorithms. All execution times per pixel have been measured in a standard PC Pentium IV with 1 GB RAM memory and 2.0 GHz clock speed. All algorithms have been implemented and executed in MATLAB 7.1, under Windows XP Pro.

Advantages	Disadvantages	Execution time / pixel
ROA Operator		
<ul style="list-style-type: none"> • Moderated computational load. • Adaptive to speckle level 	<ul style="list-style-type: none"> • Low contrast ESM. • High edge strength in speckled pixels when low window sizes are used. • High noise in detected edges when big window sizes are used. 	Minimum: 76 μ s Maximum: 305 μ s
Oliver & White Operator		
<ul style="list-style-type: none"> • High detail of the ESM in edges enclosing small regions. • Good definition in edges enclosing high reflectivity regions: good extended target detection performance. • Good performance against speckle, even when small window sizes are used. 	<ul style="list-style-type: none"> • High Pfa when small window sizes are used. • Big difference between ESM values of edges separating regions with very different average intensities than regions with near average intensities. 	Minimum: 73 μ s Maximum: 293 μ s
ROEWA Operator		
<ul style="list-style-type: none"> • Constant computational load, independently of the speckle level. • Good performance against speckle and low false alarm rates. 	<ul style="list-style-type: none"> • Excessive edge thickness in high speckle images. • Good ESM contrast only when edge shapes are so thick that region shapes are deformed. 	Minimum = Maximum: 190 μ s
RDMA Operator		
<ul style="list-style-type: none"> • Low computational load. 	<ul style="list-style-type: none"> • Extremely reduced ESM contrast, it is appreciable for window sizes that produce excessive edge thickness. • High false alarm rates. 	Minimum: 28 μ s Maximum: 210 μ s

Advantages	Disadvantages	Execution time / pixel
Madchakham algorithm		
<ul style="list-style-type: none"> • Low computational load. • ESMs with good contrast and reduced false alarms due to speckle. 	<ul style="list-style-type: none"> • High edge thickness when speckle must be mitigated. 	Minimum: 3,7 μ s Maximum: 6,2 μ s
Multiresolution ROA Operator		
<ul style="list-style-type: none"> • High configuration versatility. • High quality ESMs. Allows setting the execution to optimise jointly both edge detection and reduced false alarm rate with low edge thickness. 	<ul style="list-style-type: none"> • High computational load 	Minimum: 22 μ s Maximum: 1.0 ms

Table1: Summary of edge detection performances

4. CONCLUSIONS

Several edge detection algorithms based on the computation of the edge strength map over intensity SAR images have been evaluated and compared. Big differences have been found in terms of computational load, protection against speckle, false alarm rate and edge strength contrast. The ones based on wavelet transform have shown best performances: (a) Madchakham algorithm obtains the best execution time maintaining good performance in ESM quality. (b) Multiresolution ROA Operator algorithm has shown the best ESM performance, but at the expense of high computational load. It seems clear that the best choice between both algorithms will depend on the execution time constraints of the target application and the speckle level of the input SAR images.

The concept of ESM combination introduced in [10] and applied in this paper will be a matter of future research. Preliminary results obtained applying other ESM combination techniques have shown a promising increase in edge quality performance.

5. ACKNOWLEDGEMENTS

This work has been co-funded by Spanish MoD and Sener Ingeniería y Sistemas, in the frame of the Aerospace Division R&D program. The authors specially acknowledge the Radar Laboratory of INTA (Spanish Institute of Aerospace Techniques) for their support and the images provided from their RIX-P1 SAR system.

6. REFERECES

- [1] R. Touzi, A. Lopès and P. Bousquet, "A statistical and geometrical edge detector for SAR images", IEEE Transactions on Geoscience and Remote Sensing, vol. 26, no. 6, pp. 764-773, November 1988.
- [2] R.G. White, C.J. Oliver, "Change detection in SAR imagery", Record of the IEEE 1990 International Radar Conference, pp 217-222, May 1990.
- [3] C.J. Oliver, D. Blacknell, R.G. White, "Optimum edge detection in SAR", IEE Proceedings - Radar, Sonar and Navigation, Vol. 143, Iss. 1, pp 31-40, Feb 1996.
- [4] R. Fjørtoft, A. Lopès, P. Marthon, E. Cubero-Castan, "An optimal multiedge detector for SAR image segmentation", IEEE Transactions on Geoscience and Remote Sensing, Vol. 36, Iss. 3, pp 793-802, May 1998.
- [5] G. Oller, P. Marthon, L. Rognant, "Edge detection and extraction for SAR images", Proceedings IEEE Geoscience and Remote Sensing Symposium IGARSS '03, Vol. 6, pp 4004-4006, July 2003.
- [6] R. Fjørtoft, A. Lopès, J. Bruniquel, P. Marthon, "Optimal edge detection in SLC images with correlated speckle", 1998 IEEE International Geoscience and Remote Sensing Symposium Proceedings IGARSS '98, Vol. 1, pp 342-344, July 1998.
- [7] R. Fjørtoft, A. Lopès, J. Bruniquel, P. Marthon, "Optimal edge detection and edge localization in complex SAR images with correlated speckle", IEEE Transactions on Geoscience and Remote Sensing, Vol. 37, Iss. 5, Part 1, pp 2272-2281, Sept 1999.

- [8] M. Chabert, F. Hlawatsch, J.Y. Tournet, "Improved multiedge detection and reflectivity estimation for SAR images", IEEE International Conference on Acoustics, Speech, and Signal Processing Proceedings ICASSP '02, Vol. 2, pp 1301-1304, May 2002.
- [9] Z. Zhiqin, H. Chunlin, W. Jianguo, H. Shunji, "A new method for edge detection of SAR image", IEEE 2000 International Radar Conference, pp 551-553, 2000.
- [10] R. Fjørtoft, P. Marthon and A. Lopès, "Multiresolution edge detection in SAR images", Proceedings NORISIG, Tromsø, Norway, May 1997.
- [11] S. Madchakham, P. Thitimajshima, Y. Rangsanteri, "Edge Detection in Speckled SAR Images using Wavelet Decomposition", Proceedings ACRS 2001 - 22nd Asian Conference on Remote Sensing, Vol. 2, pp 1307-1310, Singapore, November 2001.
- [12] V. Manian, R. Vásquez, "Multiresolution edge detection algorithm applied to SAR images", Proceedings IEEE Geoscience and Remote Sensing Symposium IGARSS '99, Vol. 2, pp 1291-1293, 1999.
- [13] M. Chabert, J. Y. Tournere, and Gilles Mesnager, "Edge detection in speckled SAR images using the continuous wavelet transform", Proceedings IEEE Geoscience and Remote Sensing Symposium IGARSS'96, pp.1842-1844, May 1996.
- [14] P. Moreels, S. E. Smrekar, "Watershed identification of polygonal patterns in noisy SAR images", IEEE Trans. Image Processing, Vol. 12, Iss. 7, pp 740-750, July 2003. ([3.16]).
- [15] P. Marthon, B. Paci and E. Cubero-Castan, "Finding the structure of a satellite image", Proc. EurOpto Image and Signal Processing for Remote Sensing, vol. SPIE 2315, Rome, Italy, 1994, pp. 669-679. ([3.17]).